Acoustic band pinning in the phononic crystal plates of anti-symmetric structure*

Cai Chen(蔡 琛)[a], Zhu Xue-Feng(祝雪丰)[a], Chen Qian(陈 谦)[a], Yuan Ying(袁 樱)[b], Liang Bin(梁 彬)[a], and Cheng Jian-Chun(程建春)[a]†

[a] *Key Laboratory of Modern Acoustics, Ministry of Education, and Institute of Acoustics, Nanjing University, Nanjing* 210093, *China*

[b] *School of Mathematics and Physics, Jiangsu Teachers University of Technology, Changzhou* 213001, *China*

(Received 27 April 2011; revised manuscript received 1 June 2011)

Acoustic bands are studied numerically for a Lamb wave propagating in an anti-symmetric structure of a one-dimensional periodic plate by using the method of supercell plane-wave expansion. The results show that all the bands are pinned in pairs at the Brillouin zone boundary as long as the anti-symmetry remains and acoustic band gaps (ABGs) only appear between certain bands. In order to reveal the relationship between the band pinning and the anti-symmetry, the method of eigenmode analysis is introduced to calculate the displacement fields of different plate structures. Further, the method of harmony response analysis is employed to calculate the reference spectra to verify the accuracy of numerical calculations of acoustic band map, and both the locations and widths of ABGs in the acoustic band map are in good agreement with those of the reference spectra. The investigations show that the pinning effect is very sensitive to the anti-symmetry of periodic plates, and by introducing different types of breakages, more ABGs or narrow pass bands will appear, which is meaningful in band gap engineering.

Keywords: Lamb wave, phononic crystal, anti-symmetric structure, band structures

PACS: 63.20.–e, 62.65.+k, 43.20.+g **DOI:** 10.1088/1674-1056/20/11/116301

1. Introduction

The studies of acoustic meta-materials and phononic crystals (PCs) of different structures have been reported extensively over the past decade.[1−6] Unlike the surface acoustic wave-based PC structures that can suffer obvious loss due to coupling with the substrate, the PC plates hold better performance for implementing PC functionalities because the wave energy is totally restricted between the upper and the lower stress-free boundaries regardless of the air damping and self-dissipation. The existence of acoustic band gaps (ABGs) and the ability to confine and guide elastic waves with low loss make the PC plates excellent candidates for the implementation of acoustic resonators, filters, wave guides, etc. in chip-scale integrated wireless devices.[5−7] However, the mechanism of formation of ABGs is very complicated and still incomplete, because the elastic waves in PC plates can be scattered by not only the periodic inclusions but also the two stress-free boundaries. In general, Lamb wave modes in homogeneous plates can be separated into two independent sets: the symmetric and the anti-symmetric modes, named S and A modes, respectively. However, for plates with inclusions (periodic, quasi-periodic or random) embedded, the coupling happens between the same or different mode sets, which induces a separation or splitting of their dispersion curves.[8] Increased coupling is therefore the cause of the increased separation, which will finally lead to the formation of ABGs. Many researchers[6,7,9] have studied the formation of ABGs in different plate structures through the band structure evolution or mode coupling and shown that in PC plate with a mirror midplane, the S mode is completely decoupled with A mode so that the coupling can happen only between the same mode sets (S or A modes). However, in plate with an asymmetric midplane, the amplitude distribution of displacement field is also asymmetric

*Project supported by the National Basic Research Program of China (Grant No. 2010CB327803), the National Natural Science Foundation of China (Grant Nos. 10874086, 10834009, and 10904068), the Science Foundation of the Ministry of Education of China (Grant No. 705017), and the Fundamental Research Funds for the Central Universities, China (Grant No. 1085020401).

†Corresponding author. E-mail: jccheng@nju.edu.cn

© 2011 Chinese Physical Society and IOP Publishing Ltd

with respect to the midplane for any eigenmode, which implies that the coupling will happen between S and A modes as well. With the above-mentioned information, it is clear that the amplitude distribution of displacement field of each eigenmode is notably related to the plate structure.[9]

In this article, we first study the propagation of Lamb waves in an anti-symmetric structure of one-dimensional periodic plate by using the method of supercell plane-wave expansion. The anti-symmetric structure is characterized by the structural invariance after translating along the plate for half a lattice constant and mirroring to its midplane, which has rarely been studied elsewhere to the best of our knowledge. The results show that all the bands are pinned in pairs at the Brillouin zone boundary as long as the anti-symmetry remains and ABGs appear only between certain bands. Note that the pinning phenomenon is very common in condense physics, such as flux pinning in superconductor and Fermi level pinning in semiconductor. The acoustic band pinning is somewhat different from others in principle. Then, the eigenmode analysis is employed to reveal the relationship between the band pinning and the anti-symmetry by calculating the displacement fields of different plate structures. Finally, the method of harmony response analysis (HRA)[10] is employed to calculate the reference spectra to verify the accuracy of numerical calculations of acoustic band map, and both the locations and widths of ABGs in the acoustic band map are in good agreement with those of the reference spectra. The investigations show that the pinning effect is very sensitive to the anti-symmetry of periodic plates and, by introducing different types of breakages, more ABGs will appear, which is meaningful in band gap engineering.

The rest of the present article is organized as follows. In Section 2, the numerical model is proposed, which is employed to study the PC plates with different topological structures in a simple one-dimensional case. In Section 3, some numerical results are obtained and a topological explanation to the band pinning is given. Finally, some conclusions are drawn from the present study in Section 4.

2. Numerical model

The anti-symmetric structure of one-dimensional periodic plate is presented in Fig. 1(a) and in each unit cell, a is the lattice constant, c the horizontal shift between the two neighbouring inclusions, h_1, h_2 and b_1, b_2 the heights and the widths of the upper and the lower inclusions, respectively. Throughout the article, the lattice constant a and the plate thickness $h = h_1 + h_2$ are constants and set to be 2 mm.

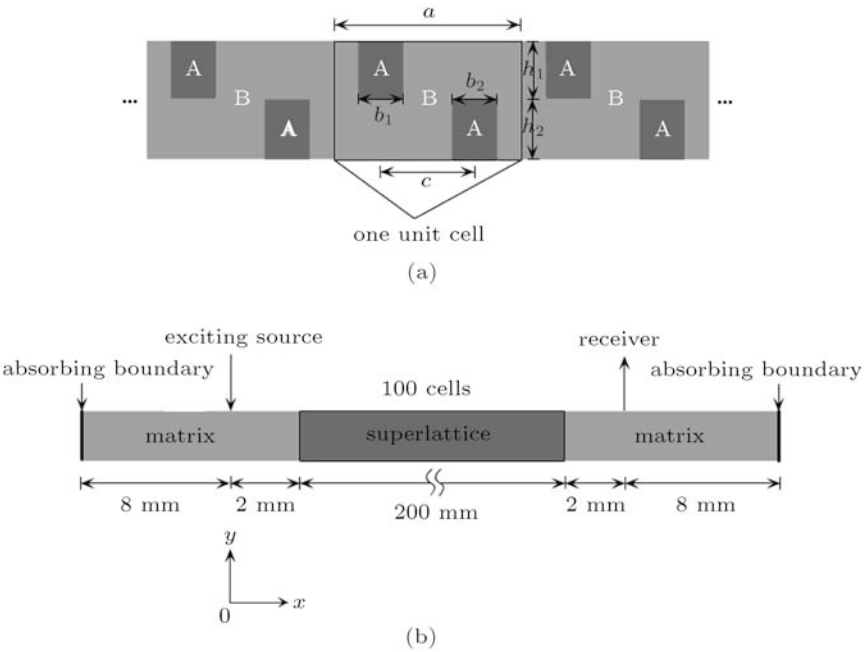


Fig. 1. (a) Scheme of the anti-symmetric structure of one-dimensional periodic plate with inclusion material A (tungsten) and matrix material B (silicon). (b) The configuration of the composite PC plate in HRA calculation, with the superlattice composed of 100 unit cells.

Figure 1(b) shows the configuration of the composite PC plate in HRA calculation. The one-dimensional PC superlattice with 100 cells of 200 mm in length is bounded by two 10-cm-long silicon matrixes on two sides. In our numerical simulations, the Lamb waves are excited at $x = 0$, $y = 2$ and received at point 2 mm away from the superlattice ($x = 204$, $y = 2$), with absorbing boundaries employed at two ends to suppress the Lamb wave reflections. The point exciting source is a harmony frequency force load and, by calculating the received displacements of the PC plate and a reference homogenous plate under different frequency loads, we can obtain the normalized transmitted power spectra directly in frequency domain. The elastic constants and the densities of the materials used in the numerical calculations are given in Ref. [11].

3. Numerical results and discussion

Acoustic band pinning is defined by the phenomenon that acoustic bands are pinned in pairs at the Brillouin zone (BZ) boundary. In order to understand the band pinning in depth, we perform a series of numerical calculations by traditional plane-wave expansion (PWE) method. Figures 2 and 3 show the band structures of the anti-symmetric plate structures with inclusions of different widths and heights, respectively. By comparison with the band structure of a homogeneous plate in Fig. 2(a), we can find that the couplings happen only between S and A modes in the lower frequency region. For example, in Fig. 2(b), mode couplings (marked by the elliptic circles) happen between A_0 and S_0, A_0 and S_1, A_1 and S_1, A_0 and S_0, separately, and in Fig. 2(c), between S_0 and A_1. In Fig. 3(b), mode couplings happen between A_0 and S_0, A_0 and S_1, A_1 and S_1, S_0 and A_1, separately, and in Fig. 3(c), between A_0 and S_0. During the band evolution [Figs. 2(a)–2(d) or 3(a)–3(c)], all the bands are pinned in pairs at the BZ boundary, which makes the ABGs exist only between certain bands. To be specific, in Fig. 2(d) or 3(c), there are four ABGs which exist between bands 2 and 3, 4 and 5, 6 and 7, 8 and 9, respectively. It is noted that the ABG between bands 2 and 3 may always exist when the inclusions of high-contrasted acoustic impedance are introduced in this anti-symmetric structure as shown in Figs. 2(b)–2(d) or 3(a)–3(c). Since it is theoretically impossible to open a gap between the bands 1 and 2, we believe that the lowest-order ABG in this anti-symmetric structure provides a low-frequency limitation for band gap engineering in the PC plates.

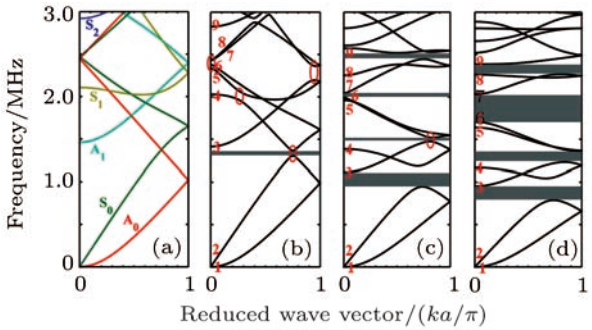


Fig. 2. (colour online) Band structures of one-dimensional periodic plates of the anti-symmetric structures with inclusions of different widths: (a) homogeneous plate, (b) $b_1 = b_2 = 0.01a$, (c) $b_1 = b_2 = 0.1a$, and (d) $b_1 = b_2 = 0.2a$; Horizontal shift $c = 0.5a$, and inclusion heights $h_1 = h_2 = 0.5h$.

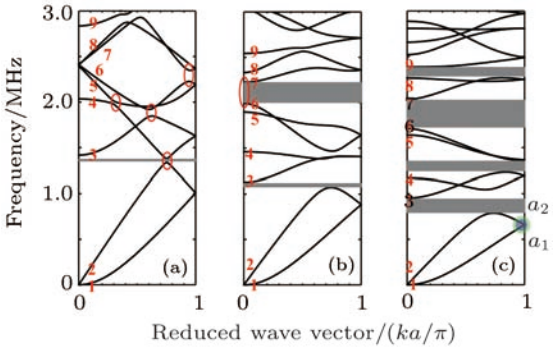


Fig. 3. (colour online) Band structures of one-dimensional periodic plates of the anti-symmetric structures with inclusions of different heights: (a) $h_1 = h_2 = 0.01h$, (b) $h_1 = h_2 = 0.5h$, and (c) $h_1 = h_2 = 0.5h$. Horizontal shift $c = 0.5a$, and inclusion widths $b_1 = b_2 = 0.2h$.

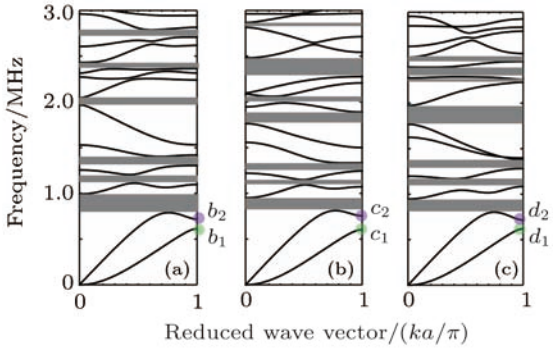


Fig. 4. (colour online) Band structures of one-dimensional periodic plates with three types of breakages (a) Type-I: $b_1 = 0.3a$, $b_2 = 0.1a$, $c = 0.5a$, and $h_1 = h_2 = 0.5h$; (b) Type-II: $b_1 = b_2 = 0.2a$, $c = 0.5a$, $h_1 = 0.75h$, and $h_2 = 0.25h$; (c) Type-III: $b_1 = b_2 = 0.2a$, $c = 0.35a$; and $h_1 = h_2 = 0.5h$.

Detailed calculation shows that the acoustic band pinning is very sensitive to the plate structure and will vanish when the plate structure is modified, which may produce more ABGs due to the opening of criss-crossing points (especially at the BZ boundary) in the band structure. For convenience in analysis, we define three modified plate structures by introducing different types of breakages, named Type-I, Type-II and Type-III breakages respectively. In Type-I breakage, the width of upper inclusion increases with decreasing ($b_1 = 0.3a$ and $b_2 = 0.1a$). In Type-II breakage, the height h_1 of upper inclusion increases with h_2 decreasing ($h_1 = 0.75h$ and $h_2 = 0.25h$). In Type-III breakage, the horizontal shift c decreases ($c = 0.35a$). For each type of breakages, we calculated the band structure as shown in Figs. 4(a)–4(c), and the results show that ABGs in the modified plates are plentiful and more complicated. To be specific, for Type-I breakage, there are six ABGs (0.788 MHz–0.991 MHz, 1.112 MHz–1.204 MHz, 1.304 MHz–1.402 MHz, 1.967 MHz–2.045 MHz, 2.364 MHz–2.431 MHz and 2.708 MHz–2.787 MHz), and the number increases to seven for Type-II and Type-III breakages (0.812 MHz–0.951 MHz, 1.093 MHz–1.149 MHz, 1.245 MHz–1.333 MHz, 1.762 MHz–1.888 MHz, 1.989 MHz–2.059 MHz, 2.276 MHz–2.480 MHz and 2.814 MHz–2.866 MHz; 0.802 MHz–0.947 MHz, 1.084 MHz–1.167 MHz, 1.281 MHz–1.379 MHz, 1.768 MHz–1.974 MHz, 2.230 MHz–2.261 MHz, 2.289 MHz–2.396 MHz, and 2.459 MHz–2.506 MHz).

In order to study the relationship between the band pinning and the plate structure intuitively, we calculate the displacement fields of eight selected eigenmodes at points a_1 and a_2 in Fig. 3(c); points b_1 and b_2 in Fig. 4(a); points c_1 and c_2 in Fig. 4(b); points d_1 and d_2 in Fig. 4(c) as shown in Figs. 5(a)–5(d) where the panels on the left-hand side show the displacement fields of the modes at points a_1, b_1, c_1, and d_1; the panels on the right-hand side show the displacement fields of the modes at points a_2, b_2, c_2, and d_2. It is clear that the amplitude distributions of displacement fields are closely related to the plate structure. When the plate structure is anti-symmetric with respect to the midplane, the displacement fields of the modes at points a_1 and a_2 are actually the same (see Fig. 5(a)) (translating one field by half a lattice constant along the plate and mirroring to the midplane, we can obtain the other), so the two modes can be regarded as the same one (see Fig. 3(c)). However, when the plate structure is modified by Type-I breakage, the displacement fields of the modes at points b_1 and b_2 are different from those in Fig. 5(b) (we can never obtain one field from the other by translating and mirroring), which means the two modes are different as shown in Fig. 4(a). The same conclusion can be obtained in Figs. 5(c) and 5(d), when the plate structure is modified by Type-II and Type-III breakages, respectively. Moreover, in the calculation of band structures by traditional PWE method, we employ the Bloch theory and the default that the period of displacement field (u) in PC plate is the same as the period of the inclusion array, which equals the lattice constant a. However, in the anti-symmetric structure, the period of displacement field (u) can be regarded as $a/2$ as mentioned above, which will lead to the band pinning at BZ boundary when we use the lattice constant a to do the Fourier expansion with respect to u in the supercell PWE method.

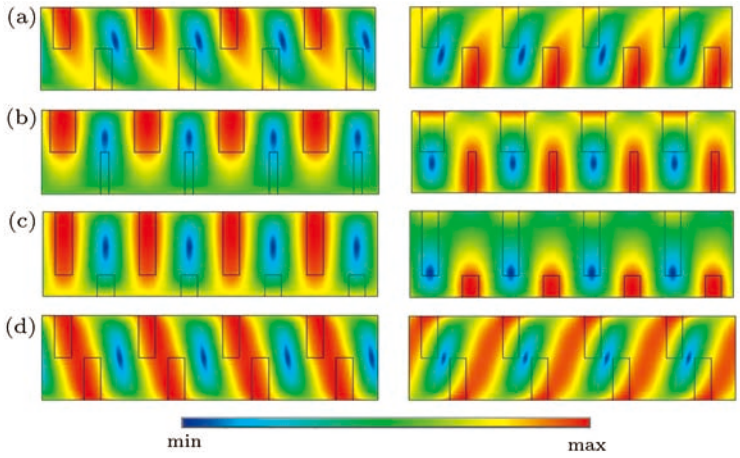


Fig. 5. (colour online) Displacement fields of eigenmodes with (a) $ka/\pi = 1$, $f_1 = 0.655$ MHz at point a_1 in Fig. 3(c), $f_2 = 0.655$ MHz at point a_2 in Fig. 3(c); (b) $ka/\pi = 1$, $f_1 = 0.613$ MHz at point b_1 in Fig. 4(a), $f_2 = 0.718$ MHz at point b_2 in Fig. 4(a); (c) $ka/\pi = 1$, $f_1 = 0.602$ MHz at point c_1 in Fig. 4(b), $f_2 = 0.754$ MHz at point c_2 in Fig. 4(b); (d) $ka/\pi = 1$, $f_1 = 0.691$ MHz at point d_1 in Fig. 4(c), $f_2 = 0.714$ MHz at point d_2 in Fig. 4(c). The left fields correspond to points a_1, b_1, c_1, d_1, respectively; the right to points a_2, b_2, c_2, d_2, respectively.

In order to demonstrate further the increase of band gaps after different types of breakages are introduced, the HRA is employed to calculate the reference spectrum which is defined by the ratio of the spectrum calculated in the PC plate to that calculated in a homogeneous plate with the same thickness (2 mm). The reference spectra of three modified plate structures are shown in Figs. 6(a)–6(c), where six obvious ABGs exist for the Type-I breakage (marked by gray bars), ranging from 0.788 MHz to 0.986 MHz, 1.112 MHz to 1.200 MHz, 1.303 MHz to 1.397 MHz, 1.967 MHz to 2.060 MHz, 2.395 MHz to 2.445 MHz, and 2.740 MHz to 2.807 MHz, respectively, and the gap number increases to seven for Type-II and Type-III breakages (0.814 MHz–0.951 MHz, 1.093 MHz–1.147 MHz, 1.243 MHz–1.327 MHz, 1.791 MHz–1.888 MHz, 1.990 MHz–2.060 MHz, 2.289 MHz–2.503 MHz and 2.825 MHz–2.906 MHz; 0.806 MHz–0.947 MHz, 1.080 MHz–1.166 MHz, 1.277 MHz–1.371 MHz, 1.768 MHz–1.980 MHz, 2.237 MHz–2.289 MHz, 2.314 MHz–2.409 MHz, and 2.460 MHz–2.546 MHz), which is consistent with the results in the band structure calculation as shown in Figs. 4(a)–4(c).

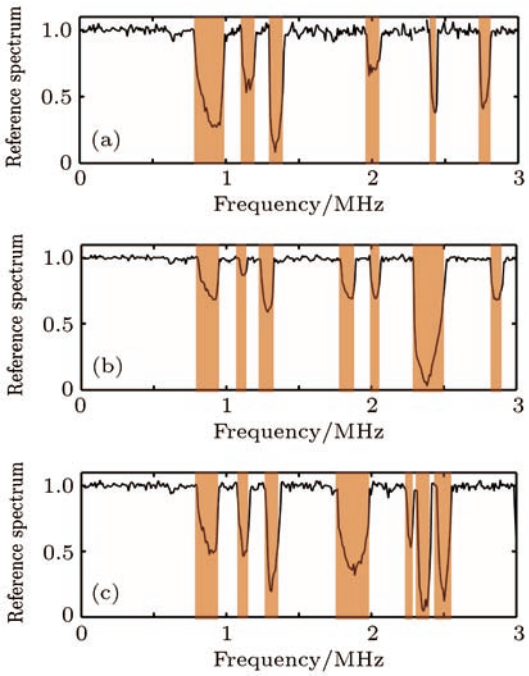


Fig. 6. (colour online) Reference spectra of one-dimensional periodic plates with three types of breakages (a) Type-I: $b_1 = 0.3a$, $b_2 = 0.1a$, $c = 0.5a$ and $h_1 = h_2 = 0.5h$; (b) Type-II: $b_1 = b_2 = 0.2a$, $c = 0.5a$, $h_1 = 0.75h$ and $h_2 = 0.25h$; (c) Type-III: $b_1 = b_2 = 0.2a$, $c = 0.35a$ and $h_1 = h_2 = 0.5h$.

4. Conclusion

We demonstrated the existence of acoustic band pinning in an anti-symmetric structure of one-dimensional PC plate, which is defined by the phenomenon that all the bands are pinned in pairs at the BZ boundary. Band structures of different PC plates were calculated by supercell PWE, in which the pinning phenomenon is clearly observed for the anti-symmetric structure and the couplings can occur only between S and A modes in the lower frequency region. However, with three types of breakages introduced into this structure, the band pinning instantly vanishes and the couplings happen between the same mode sets as well, which may produce more ABGs or narrow pass bands. Using eigenmode analysis, we revealed the close relationship between band pinning and plate structure and pointed out that the pinning phenomenon can exist only in the PC plates of anti-symmetric structures. Finally, the reference spectra of different PC plates were calculated by HRA, which are consistent with the band structures in the locations and widths of band gaps. Those characteristics based on the band pinning provide much significance in the application of Lamb wave insulation or filtering.

References

[1] Zhu X F, Liang B, Kan W W, Zou X Y and Cheng J C 2011 *Phys. Rev. Lett.* **106** 014301

[2] Zhao H G, Wen J H, Liu Y Z, Yu D L, Wang G and Wen X S 2008 *Chin. Phys.* B **17** 1305

[3] Zhu X F, Liu S C, Xu T, Wang T H and Cheng J C 2010 *Chin. Phys.* B **19** 044301

[4] Zhu X F, Zou X Y, Liang B and Cheng J C 2010 *J. Appl. Phys.* **108** 124909

[5] Mohammadi S, Eftekhar A A, Khelif A, Hunt W D and Adibi A 2009 *Appl. Phys. Lett.* **94** 051906

[6] Wu T T, Huang Z G, Tsai T C and Wu T C 2008 *Appl. Phys. Lett.* **93** 111902

[7] Wu T C, Wu T T and Hsu J C 2009 *Phys. Rev.* B **79** 104306

[8] Wu T T and Huang Z G 2004 *Phys. Rev.* B **70** 214304

[9] Hou Z L and Assouar B M 2008 *J. Phys.* D: *Appl. Phys.* **41** 215102

[10] Zhu X F, Xu T, Liu S C and Cheng J C 2009 *J. Appl. Phys.* **106** 104901

[11] Elastic constants $C_{\rm A}^{11} = 50.20 \times 10^{10}$, $C_{\rm A}^{12} = 19.90 \times 10^{10}$, $C_{\rm A}^{44} = 15.20 \times 10^{10}$ (in units of N/m^2), and mass density $\rho = 19200$ kg/m^3 for tungsten. Elastic constants $C_{\rm B}^{11} = 16.57 \times 10^{10}$, $C_{\rm B}^{12} = 6.390 \times 10^{10}$, $C_{\rm B}^{44} = 7.956 \times 10^{10}$ (in units of N/m^2), and mass density $\rho = 2332$ kg/m^3 for silicon.